Inorganic Chemistry
Article

Inorg. Chem. **2011**, *50*, 1351–1360 **1351**
DOI: 10.1021/ic101956z

Binuclear Methylborole Iron Carbonyls: Iron−Iron Multiple Bonds and Perpendicular Structures

Jianlin Chen,[†] Shaolin Chen,[†] Liu Zhong,[†] Hao Feng,*[,†] Yaoming Xie,[‡] and R. Bruce King*[,†,‡]

[†]*School of Physics and Chemistry, Research Center for Advanced Computation, Xihua University, Chengdu, China 610039, and* [‡]*Department of Chemistry and Center for Computational Chemistry, University of Georgia, Athens, Georgia 30602, United States*

Received September 24, 2010

Methylborole iron tricarbonyl, $(\eta^5\text{-}C_4H_4BCH_3)Fe(CO)_3$, is known experimentally and is a potential source of binuclear $(C_4H_4BCH_3)_2Fe_2(CO)_n$ ($n = 5, 4, 3, 2, 1$) derivatives through reactions such as photolysis. In this connection the lowest energy $(C_4H_4BCH_3)_2Fe_2(CO)_5$ structures are predicted theoretically to have a single bridging carbonyl group and Fe−Fe distances consistent with formal single bonds. The lowest energy $(C_4H_4BCH_3)_2Fe_2(CO)_4$ structures have two bridging carbonyl groups and Fe═Fe distances suggesting formal double bonds. Analogously, the lowest energy $(C_4H_4BCH_3)_2Fe_2(CO)_3$ structures have three bridging carbonyl groups and very short Fe≡Fe distances suggesting formal triple bonds. The tetracarbonyl $(C_4H_4BCH_3)_2Fe_2(CO)_4$ is predicted to be thermodynamically unstable toward disproportionation into $(C_4H_4BCH_3)_2Fe_2(CO)_5 + (C_4H_4BCH_3)_2Fe_2(CO)_3$, whereas the tricarbonyl is thermodynamically viable toward analogous disproportionation. The lowest energy structures of the more highly unsaturated methylborole iron carbonyls $(C_4H_4BCH_3)_2Fe_2(CO)_n$ ($n = 2, 1$) have hydrogen atoms bridging an iron−carbon bond. In addition, the lowest energy $(C_4H_4BCH_3)_2Fe_2(CO)$ structures are "slipped perpendicular" structures with bridging methylborole ligands, a terminal carbonyl group, and agostic $CH_3 \rightarrow Fe$ interactions involving the methyl hydrogens. Thus, in these highly unsaturated systems the methyl substituent in the methylborole ligand chosen in this work is not an "innocent bystander" but instead participates in the metal−ligand bonding.

1. Introduction

The landmark discovery of the sandwich compound ferrocene,[1,2] $(\eta^5\text{-}C_5H_5)_2Fe$, in 1951 stimulated the rapid subsequent development of transition metal organometallic chemistry, particularly the chemistry of cyclopentadienylmetal derivatives. In this connection, the first cyclopentadienylmetal derivatives to be discovered include the sandwich compounds $(\eta^5\text{-}C_5H_5)_2M$ of the first row transition metals (M = V, Cr, Mn, Fe, Co, Ni), as well as stable cyclopentadienylmetal carbonyl derivatives of these metals. Among the most stable of these originally discovered cyclopentadienylmetal carbonyls is the manganese derivative $(\eta^5\text{-}C_5H_5)Mn(CO)_3$, commonly known as cymantrene.[3,4] The cymantrene unit is stable enough to allow organic transformations to be performed on the $\eta^5\text{-}C_5H_5$ ring without disturbing the $Mn(CO)_3$ moiety. Also, methylcymantrene, $(\eta^5\text{-}MeC_5H_4)Mn(CO)_3$, is stable enough to have been used as a lead-free antiknock derivative in gasoline and related fuels[5] until environmental considerations caused any metal-containing gasoline additives to be phased out of use.

The development of the transition metal chemistry of heterocycles related to the cyclopentadienyl ligand occurred considerably later, owing to initial synthetic challenges in obtaining the required heterocyclic starting materials. Replacing one of the five carbon atoms in the neutral cyclopentadienyl ligand with boron gives the borole ligand, C_4H_4BH, which has one electron less than the cyclopentadienyl ligand (Figure 1). As a result, the neutral borole ligand is a net donor of only four π electrons whereas a neutral cyclopentadienyl ligand is a net donor of five π electrons. In this respect a neutral borole ligand is related to a neutral cyclobutadiene ligand. However, a borole ligand can function as a pentahapto $\eta^5\text{-}C_4H_4BH$ ligand with the boron atom as well as the four carbon atoms within bonding distance of a transition metal. This contrasts with the cyclobutadiene ligand, which obviously can function only as a tetrahapto $\eta^4\text{-}C_4H_4$ ligand.

The possibilities for the synthesis of metal borole complexes are limited by the instability of most boroles. Thus borole, like cyclobutadiene, is a 4π electron antiaromatic system[6] and thus

*To whom correspondence should be addressed. E-mail: fenghao@mail.xhu.edu.cn (H.F.), rbking@chem.uga.edu (R.B.K.).

(1) Kealy, T. J.; Pauson, P. L. *Nature* **1961**, *168*, 1039.
(2) Miller, S. A.; Tebboth, J. A.; Tremaine, J. F. *J. Chem. Soc.* **1952**, 632.
(3) Fischer, E. O.; Jira, R. *Z. Naturforsch.* **1954**, *9b*, 618.
(4) Piper, T. S.; Cotton, F. A.; Wilkinson, G. *J. Inorg. Nucl. Chem.* **1955**, *1*, 165.
(5) Hollrah, D. P.; Burns, A. M. *Oil Gas J.* **1991**, *89*, 86.

Published on Web 01/21/2011

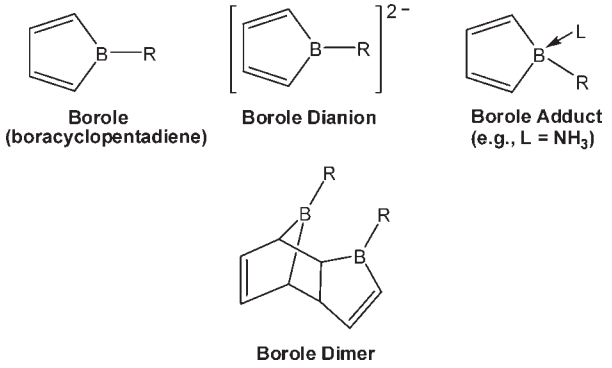

Figure 1. Boroles, their dianions, their adducts with Lewis bases, and their dimers. In the reported experimental work[15] typical R groups are methyl and phenyl.

not expected to be stable in the free state. Stable boroles can only be obtained if most or all of the hydrogen atoms are replaced by larger substituents. In this connection, the first borole to be synthesized was pentaphenylborole[6−8] $(C_6H_5)_4C_4BC_6H_5$, which was found to be highly reactive consistent with its antiaromaticity. Other pentaarylboroles were subsequently synthesized.[9,10] Such boroles are of interest as extremely strong Lewis acids for use in olefin polymerization catalysts, as shown recently by Tilley and co-workers.[11] In addition, boroles provide rare examples of transition metal-free systems that can activate dihydrogen.[12] Uncomplexed monomeric boroles with small groups on the carbon atoms have also been shown to be unstable with respect to Diels−Alder dimerization,[13] similar to the conversion of monomeric cyclopentadiene to dicyclopentadiene (Figure 1).[9] However, such boroles can be stabilized by complexation with ammonia (Figure 1).[14] In addition boroles can be reduced to stable dianions[10] $[R_4C_4BR']^{2-}$ (R and R′ = phenyl or other aryl groups). These dianions are stable 6π electron systems isoelectronic with the cyclopentadienyl anion.

The instability of most boroles limits their use as reagents for the synthesis of their transition metal complexes. Fortunately, indirect methods have been found providing methods for the synthesis of borole metal complexes without a need for the free borole. The most useful such method uses the fact that whereas most boroles are unstable antiaromatic systems, their dihydro derivatives (borolenes) are stable and undergo dehydrogenation upon thermal reactions with many metal carbonyls to give borole metal carbonyl complexes. Examples of borole metal carbonyl complexes that have been prepared in this manner include the mononuclear $(\eta^5\text{-}C_4H_4BR)M(CO)_3$

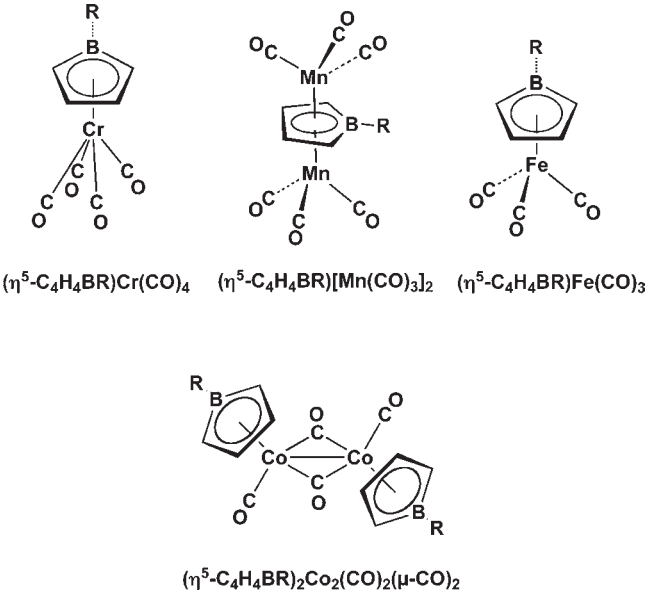

Figure 2. Examples of borole metal carbonyls.

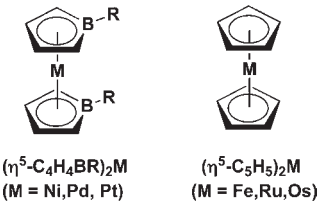

Figure 3. Comparison of the isoelectronic bis(borole) sandwich compounds $(\eta^5\text{-}C_4H_4BR)_2M$ (M = Ni, Pd, Pt) and bis(cyclopentadienyl) sandwich compounds $(\eta^5\text{-}C_5H_5)_2M$ (M = Fe, Ru, Os).

(M = Fe,[15] Ru,[16] Os;[16] R = CH_3, C_6H_5), the binuclear $(\eta^5\text{-}C_4H_4BR)_2Co_2(CO)_2(\mu\text{-}CO)_2$,[15] and the triple-decker sandwich[15] $(\eta^5,\eta^5\text{-}\mu\text{-}C_4H_4BR)[Mn(CO)_3]_2$ with a bridging borolyl ligand (Figure 2).[15] In addition, boroles can be stabilized as ammonia adducts $C_4H_4BR\cdot NH_3$, which are generated from degradation of the cobalt carbonyl derivatives $(\eta^5\text{-}C_4H_4BR)Co(CO)_2I$ with ammonia.[14] Reactions of such borole ammonia adducts with the tetrahydrofuran complexes $(thf)M(CO)_5$ (M = Cr, Mo, W) generate the corresponding metal carbonyl derivatives $(\eta^5\text{-}C_4H_4BR)M(CO)_4$ (Figure 2).[14] The borole ammonia adducts also react with the 1,5-cyclooctadiene complexes $(1,5\text{-}C_8H_{12})_2M$ (M = Ni, Pd, Pt) to form $(1,5\text{-}C_8H_{12})M(\eta^5\text{-}C_4H_4BR)$, which upon pyrolysis give the sandwich compounds[17] $(\eta^5\text{-}C_4H_4BR)_2M$. These sandwich compounds (Figure 3) are isoelectronic with the well-known very stable metallocenes $(\eta^5\text{-}C_5H_5)_2M$ (M = Fe, Ru, Os).

Among the most stable and readily synthesized borole metal carbonyl complexes are the iron derivatives[15] $(\eta^5\text{-}C_4H_4BR)Fe(CO)_3$. These are isoelectronic with both cymantrene $(\eta^5\text{-}C_5H_5)Mn(CO)_3$ and the very stable cyclobutadiene-iron tricarbonyl $(\eta^4\text{-}C_4H_4)Fe(CO)_3$. Both of these latter systems are known to undergo photolysis to form binuclear derivatives with metal−metal bonds. Among such derivatives, the binuclear tricarbonyls[18−21] $(\eta^5\text{-}C_5H_5)_2Mn_2(CO)_3$ and $(\eta^4\text{-}C_4H_4)_2Fe_2(CO)_3$

(6) Braunschweig, H.; Fernandez, I.; Frenking, G.; Kupfer, T. *Angew. Chem., Int. Ed.* **2008**, *47*, 1951.
(7) Eisch, J. J.; Hota, N. K.; Kosima, S. *J. Am. Chem. Soc.* **1969**, *91*, 4575.
(8) Eisch, J. J.; Galle, J. E.; Kozima, S. *J. Am. Chem. Soc.* **1986**, *108*, 379.
(9) Fagan, P. J.; Burns, E. G.; Calabrese, J. C. *J. Am. Chem. Soc.* **1988**, *110*, 2979.
(10) So, C.-W.; Watanabe, D.; Wakamiya, A.; Yamaguchi, S. *Organometallics* **2008**, *27*, 3496.
(11) Huynh, K.; Vigneille, J.; Tilley, T. D. *Angew. Chem., Int. Ed.* **2009**, *48*, 2835.
(12) Fan, C.; Mercier, L. G.; Piers, W. E.; Tuononen, H. M.; Parvez, M. *J. Am. Chem. Soc.* **2010**, *132*, 9604.
(13) Fagan, P. J.; Nugent, W. A.; Calabrese, J. C. *J. Am. Chem. Soc.* **1994**, *116*, 1880.
(14) Herberich, G. E.; Hessner, B.; Negele, M.; Howard, J. A. K. *J. Organomet. Chem.* **1987**, *336*, 29.
(15) Herberich, G. E.; Boveleth, W.; Hessner, B.; Köffer, D. P. J.; Negele, M.; Saive, R. *J. Organomet. Chem.* **1986**, *308*, 153.
(16) Herberich, G. E.; Boveleth, W.; Hessner, B.; Hostaler, M.; Köffer, D. F. J.; Negele, M. *J. Organomet. Chem.* **1987**, *319*, 311.
(17) Herberich, G. E.; Negele, M. *J. Organomet. Chem.* **1988**, *350*, 81.
(18) Herrmann, W. A.; Serrano, R.; Weichmann, J. *J. Organomet. Chem.* **1983**, *246*, C57.
(19) Bernal, I.; Korp, J. D.; Hermann, W. A.; Serrano, R. *Chem. Ber.* **1984**, *117*, 434.

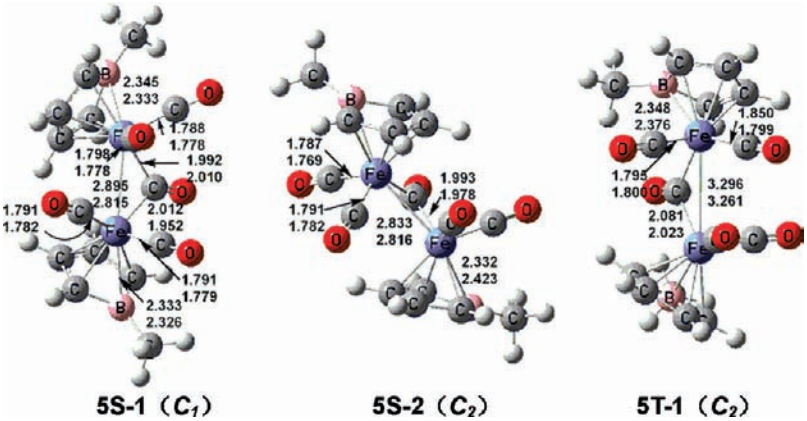

Figure 4. Optimized geometries for the three $(C_4H_4BCH_3)_2Fe_2(CO)_5$ structures. In Figures 4 to 8, the upper bond distances (in Å) are predicted by B3LYP, and the lower bond distances are predicted by BP86.

Table 1. Total Energies (E in a.u.), Relative Energies (ΔE in kcal/mol), Fe−Fe and Fe−B Distances (in Å), Numbers of Imaginary Vibrational Frequencies (Nimg), and Spin Expectation Values $\langle S^2 \rangle$ for the $(C_4H_4BCH_3)_2Fe_2(CO)_5$ Structures

	5S-1 (C_1)		**5S-2** (C_2)		**5T-1** (C_2)	
	B3LYP	BP86	B3LYP	BP86	B3LYP	BP86
Fe_1-B_1	2.333	2.326	2.332	2.423	2.348	2.376
Fe_2-B_2	2.345	2.333	2.332	2.423	2.348	2.376
Fe_1-Fe_2	2.895	2.815	2.833	2.816	3.296	3.261
$-E$	3533.62042	3534.09838	3533.62929	3534.09419	3533.56406	3534.04021
ΔE	0.0	0.0	−5.6	2.6	35.4	36.5
Nimg	none	none	none	none	1 (18*i*)	2 (58*i*,26*i*)
$\langle S^2 \rangle$	0.00	0.00	0.00	0.00	2.16	2.03

with formal metal−metal triple bonds appear to be the most stable and are readily synthesized. The research reported in this paper uses density functional theory (DFT) to explore the potential of analogous binuclear methylborole complexes $(\eta^5\text{-}C_4H_4BCH_3)_2Fe_2(CO)_n$ ($n = 5, 4, 3, 2, 1$). Methylborole derivatives were chosen for this study since the potential precursor to such compounds, namely, $(\eta^5\text{-}C_4H_4BCH_3)Fe(CO)_3$, is the simplest borole iron carbonyl derivative that has been synthesized.[15]

2. Theoretical Methods

Electron correlation effects were considered by employing DFT methods, which have evolved as a practical and effective computational tool, especially for organometallic compounds.[22−36] Thus, two DFT methods were used in this study. The first functional is the B3LYP method, which is the hybrid HF/DFT method using the combination of the three parameter Becke functional (B3) with the Lee−Yang−Parr (LYP) generalized gradient correlation functional.[37,38] The other DFT method used in the present paper is BP86, which combines Becke's 1988 exchange functional (B) with Perdew's 1986 gradient corrected correlation functional method (P86).[39,40] It has been noted elsewhere that the BP86 method may be somewhat more reliable than B3LYP for the type of organometallic systems considered in this paper.[41−43] In the present study, the B3LYP and BP86 methods agree with each other fairly well in predicting the structural characteristics of the $(C_4H_4BCH_3)_2Fe_2(CO)_n$ derivatives of interest. Although both the B3LYP and BP86 results are shown in the figures and tables, unless specifically noted, only the BP86 results (geometries, energies, and vibrational frequencies) are discussed in the text.

All computations were performed using the double-ζ plus polarization (DZP) basis sets. The DZP basis sets used for boron, carbon, and oxygen add one set of pure spherical harmonic d functions with orbital exponents $\alpha_d(B) = 0.70$, $\alpha_d(C) = 0.75$, and $\alpha_d(O) = 0.85$ to the standard Huzinaga−Dunning contracted DZ sets[44,45] and are designated (9s5p1d/4s2p1d). For hydrogen, a set of p polarization functions

(20) Fischler, I.Hildenbrand, K.; von Gustorf, E. K. *Angew. Chem.* **1975**, *87*, 35.
(21) Herrmann, W. A.; Barnes, C. E.; Serrano, R.; Koumbouris, B. *J. Organomet. Chem.* **1983**, *256*, C30.
(22) Ehlers, A. W.; Frenking, G. *J. Am. Chem. Soc.* **1994**, *116*, 1514.
(23) Delley, B.; Wrinn, M.; Lüthi, H. P. *J. Chem. Phys.* **1994**, *100*, 5785.
(24) Li, J.; Schreckenbach, G.; Ziegler, T. *J. Am. Chem. Soc.* **1995**, *117*, 486.
(25) Jonas, V.; Thiel, W. *J. Phys. Chem.* **1995**, *102*, 8474.
(26) Barckholtz, T. A.; Bursten, B. E. *J. Am. Chem. Soc.* **1998**, *120*, 1926.
(27) Niu, S.; Hall, M. B. *Chem. Rev.* **2000**, *100*, 353.
(28) Macchi, P.; Sironi, A. *Coord. Chem. Rev.* **2003**, *238*, 383.
(29) Bühl, M.; Kabrede, H. *J. Chem. Theory Comput.* **2006**, *2*, 1282.
(30) Tonner, R.; Heydenrych, G.; Frenking, G. *J. Am. Chem. Soc.* **2008**, *130*, 8952.
(31) Ziegler, T.; Autschbach, J. *Chem. Rev.* **2005**, *105*, 2695.
(32) Waller, M. P.; Bühl, M.; Geethanakshmi, K. R.; Wang, D.; Thiel, W. *Chem.—Eur. J.* **2007**, *13*, 4723.
(33) Hayes, P. G.; Beddie, C.; Hall, M. B.; Waterman, R.; Tilley, T. D. *J. Am. Chem. Soc.* **2006**, *128*, 428.
(34) Bühl, M.; Reimann, C.; Pantazis, D. A.; Bredow, T.; Neese, F. *J. Chem. Theory Comput.* **2008**, *4*, 1449.
(35) Besora, M.; Carreon-Macedo, J.-L.; Cowan, J.; George, M. W.; Harvey, J. N.; Portius, P.; Ronayne, K. L.; Sun, X.-Z.; Towrie, M. *J. Am. Chem. Soc.* **2009**, *131*, 3583.
(36) Ye, S.; Tuttle, T.; Bill, E.; Simkhorich, L.; Gross, Z.; Thiel, W.; Neese, F. *Chem.—Eur. J.* **2008**, *14*, 10839.
(37) Becke, A. D. *J. Chem. Phys.* **1993**, *98*, 5648.
(38) Lee, C.; Yang, W.; Parr, R. G. *Phys. Rev. B* **1988**, *37*, 785.
(39) Becke, A. D. *Phys. Rev. A* **1988**, *38*, 3098.
(40) Perdew, J. P. *Phys. Rev. B* **1986**, *33*, 8822.
(41) See especially: Furche, F.; Perdew, J. P. *J. Chem. Phys.* **2006**, *124*, 044103.
(42) Wang, H. Y.; Xie, Y.; King, R. B.; Schaefer, H. F. *J. Am. Chem. Soc.* **2005**, *127*, 11646.
(43) Wang, H. Y.; Xie, Y.; King, R. B.; Schaefer, H. F. *J. Am. Chem. Soc.* **2006**, *128*, 11376.
(44) Dunning, T. H. *J. Chem. Phys.* **1970**, *53*, 2823.

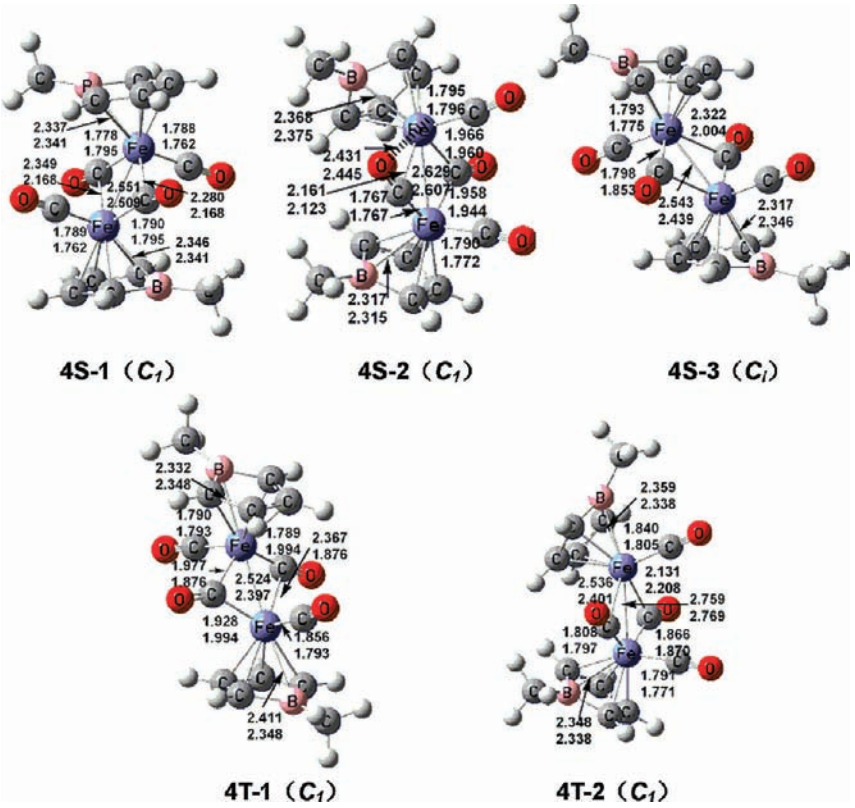

Figure 5. Optimized geometries for the five $(C_4H_4BCH_3)_2Fe_2(CO)_4$ structures.

Table 2. Total Energies (E in a.u.), Relative Energies (ΔE in kcal/mol), Fe−Fe, Fe−B Distances (in Å), Numbers of Imaginary Vibrational Frequencies (Nimg), and Spin Expectation Values $\langle S^2 \rangle$ for the $(C_4H_4BCH_3)_2Fe_2(CO)_4$ Structures

	4S-1 (C_1)		**4S-2** (C_1)		**4S-3** (C_i)	
	B3LYP(C_1)	BP86(C_i)	B3LYP	BP86(C_i)	B3LYP	BP86
Fe_1-B_1	2.337	2.341	2.368	2.375	2.317	2.346
Fe_2-B_2	2.346	2.341	2.317	2.315	2.317	2.346
Fe_1-Fe_2	2.551	2.509	2.629	2.607	2.543	2.439
$-E$	3420.24895	3420.72021	3420.24818	3420.71999	3420.24246	3420.71389
ΔE	0.0	0.0	0.5	0.1	4.1	4.0
Nimg	none	none	none	none	none	none

	4T-1 (C_1)		**4T-2** (C_1)	
	B3LYP	BP86(C_i)	B3LYP	BP86
Fe_1-B_1	2.332	2.348	2.348	2.338
Fe_2-B_2	2.411	2.348	2.359	2.338
Fe_1-Fe_2	2.524	2.397	2.759	2.679
$-E$	3420.25600	3420.71913	3420.25248	3420.70148
ΔE	−4.4	0.7	−2.2	11.7
Nimg	none	none	none	none
$\langle S^2 \rangle$	2.13	2.03	2.19	2.04

$\alpha_p(H) = 0.75$ is added to the Huzinaga−Dunning DZ set. The loosely contracted DZP basis set for iron is the Wachters primitive set[46] augmented by two sets of p functions and a set of d functions, contracted following Hood, Pitzer, and Schaefer,[47] designated (14s11p6d/10s8p3d). The geometries of all structures were fully optimized using the DZP B3LYP and DZP BP86 methods. The vibrational frequencies were determined by evaluating analytically the second derivatives of the energy with respect to the nuclear coordinates. The corresponding infrared intensities were also evaluated analytically. The ν(CO) frequencies listed in the tables were obtained by the BP86 method, which has been shown to give values closer to experimental values without using any scaling factors.[48,49] All optimizations were carried out using the Gaussian 09 program[50] with the fine grid option (75 radial shells, 302 angular points) for evaluating integrals numerically.[51]

(45) Huzinaga, S. *J. Chem. Phys.* **1965**, *42*, 1293.
(46) Wachters, A. J. H. *J. Chem. Phys.* **1970**, *52*, 1033.
(47) Hood, D. M.; Pitzer, R. M.; Schaefer, H. F. *J. Chem. Phys.* **1979**, *71*, 705.
(48) Jonas, V.; Thiel, W. *J. Phys. Chem.* **1995**, *102*, 8474.
(49) Silaghi-Dumitrescu, I.; Bitterwolf, T. E.; King, R. B. *J. Am. Chem. Soc.* **2006**, *128*, 5342.
(50) Frisch, M. J.; , et al. *Gaussian 09*, Revision A.02; Gaussian, Inc.: Wallingford, CT, 2009.
(51) Papas, B. N.; Schaefer, H. F. *J. Mol. Struct.* (*THEOCHEM*) **2006**, *768*, 175.

Unless otherwise indicated, the optimized structures are genuine minima with no imaginary vibrational frequencies.

3. Results and Discussion

3.1. Molecular Structures. 3.1.1. $(C_4H_4BCH_3)_2Fe_2(CO)_5$. Two singlet structures **5S-1** and **5S-2** and one triplet structure **5T-1** of $(C_4H_4BCH_3)_2Fe_2(CO)_5$ (Figure 4 and Table 1) are found by the B3LYP and BP86 methods. All of these structures have one bridging CO group and four terminal CO groups, that is, $(C_4H_4BCH_3)_2Fe_2(CO)_4(\mu\text{-CO})$.

The $(C_4H_4BCH_3)_2Fe_2(CO)_5$ structures **5S-1** and **5S-2** are genuine minima with no imaginary vibrational frequencies. Both structures have similar geometries (Figure 4 and Table 1). Structure **5S-1** is a cis structure, while structure **5S-2** is a trans structure in terms of the arrangement of the two borole ligands. The relative energies of these two structures depend on the method. The B3LYP method predicts **5S-2** (C_2) to be the global minimum, lying 5.6 kcal/mol below **5S-1**, while the BP86 method predicts **5S-1** to have the lower energy, lying 2.6 kcal/mol below **5S-2**. The Fe−Fe distances in **5S-1** and **5S-2** fall in the range 2.815 to 2.895 Å, consistent with the formal single bonds required to give each iron atom the favored 18-electron configuration.

The C_2 triplet $(C_4H_4BCH_3)_2Fe_2(CO)_5$ structure **5T-1** is of very high energy, lying 35.4 kcal/mol above **5S-2** (B3LYP) or 36.5 kcal/mol above **5S-1** (BP86) (Figure 4 and Table 1). Structure **5T-1** has a small imaginary vibrational frequency of $18i\ cm^{-1}$ (B3LYP) or $58i$ and $26i\ cm^{-1}$ (BP86). The Fe···Fe distance in **5T-1** is long at 3.296 Å (B3LYP) or 3.261 Å (BP86), suggesting no significant iron−iron interaction. This gives each iron atom in **5T-1** the 17-electron configuration for a binuclear triplet.

The ν(CO) frequencies for the $(C_4H_4BCH_3)_2Fe_2(CO)_5$ structures predicted using the BP86 method are listed in Table S49 of the Supporting Information. The terminal ν(CO) frequencies fall in the range 1937 to 2023 cm^{-1}. The bridging ν(CO) frequencies for the singlet structures **5S-1** and **5S-2** fall in the $1823 \pm 1\ cm^{-1}$ range. However, the ν(CO) frequency for the triplet structure **5T-1** is significantly lower at 1757 cm^{-1}. This suggests stronger $\pi \rightarrow \pi^*$ backbonding to the bridging carbonyl in the absence of a formal iron−iron bond.

3.1.2. $(C_4H_4BCH_3)_2Fe_2(CO)_4$. A total of five structures for $(C_4H_4BCH_3)_2Fe_2(CO)_4$ (three singlets and two triplets) have been optimized by both DFT methods (Figure 5 and Table 2). All of these structures are predicted to be genuine minima with no imaginary vibrational frequencies. The global minimum is dependent on the DFT method. The B3LYP method predicts **4T-1** to have the lowest energy (4.4 kcal/mol below **4S-1**). However, the BP86 method predicts **4S-1** to have the lowest energy (0.7 kcal/mol below **4T-1**). This is another example of the tendency of the B3LYP method to favor higher spin states relative to the BP86 method.[52]

All of the singlet $(C_4H_4BCH_3)_2Fe_2(CO)_4$ structures lie within 5 kcal/mol of energy and have similar geometries with two bridging CO groups, suggesting a fluxional system (Figure 5 and Table 2). Structure **4S-1** and **4S-3** are trans structures, while **4S-2** is a cis structure with respect to the orientation of the methylborole ligands. The Fe═Fe

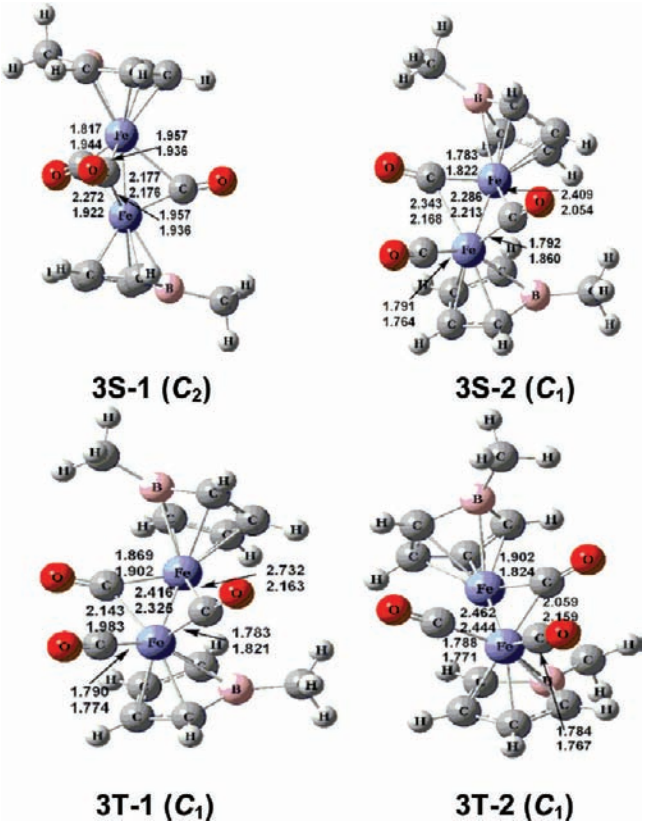

Figure 6. Optimized geometries for the four $(C_4H_4BCH_3)_2Fe_2(CO)_3$ structures.

distances of **4S-1** and **4S-3** are 2.551 Å and 2.543 Å (B3LYP) or 2.509 Å and 2.439 Å (BP86), respectively, suggesting the formal double bond required to give the iron atoms the favored 18-election configuration. The singlet structure **4S-2** has a significantly longer Fe−Fe distance, 2.629 Å (B3LYP) or 2.607 Å (BP86), consistent with a formal single bond. However, in **4S-2** there is a short Fe−O distance of 2.431 Å (B3LYP) or 2.445 Å (BP86) to one of the bridging CO groups, indicating that this CO group is a four-electron donor η^2-μ-CO group. This gives both iron atoms in **4S-2** the favored 18-electron configuration, even with a formal Fe−Fe single bond.

The triplet $(C_4H_4BCH_3)_2Fe_2(CO)_4$ structure **4T-1** is a doubly bridged trans structure (Figure 5 and Table 2). The Fe═Fe distance of 2.524 Å (B3LYP) or 2.397 Å (BP86) is consistent with a $\sigma + {}^2/_2\,\pi$ Fe═Fe double bond analogous to that in singlet dioxygen or in the binuclear iron complex[53−55] $(\eta^5\text{-}Me_5C_5)_2Fe_2(\mu\text{-CO})_3$. Thus in **4T-1** each of the two unpaired electrons of the triplet are located in separate orthogonal π orbitals leading to two π "half-bonds." This leads to the favored 18-electron configuration for each of the iron atoms.

The other triplet $(C_4H_4BCH_3)_2Fe_2(CO)_4$ structure **4T-2** is a cis singly bridged structure (Figure 5 and Table 2). The Fe→Fe distance is 2.759 Å (BP86), consistent with a Fe→Fe dative single bond from the $(C_4H_4BCH_3)Fe(CO)_2$ iron to the $(C_4H_4BCH_3)Fe(CO)$ iron. This gives each iron

(52) Reiher, M.; Salomon, O.; Hess, B. A. *Theor. Chem. Acc.* **2001**, *107*, 48.

(53) Hepp, A. F.; Blaha, J. P.; Lewis, C.; Wrighton, M. S. *Organometallics* **1984**, *3*, 174.

(54) Caspar, J. V.; Meyer, T. J. *J. Am. Chem. Soc.* **1980**, *102*, 7794.

(55) Hooker, R. H.; Mahmoud, K. A.; Rest, A. J. *Chem. Commun.* **1983**, 1022.

Table 3. Total Energies (E in a.u.), Relative Energies (ΔE in kcal/mol), Fe−Fe and Fe−B Distances (in Å), Numbers of Imaginary Vibrational Frequencies (Nimg), and Spin Contaminations $\langle S^2 \rangle$ for the $(C_4H_4BCH_3)_2Fe_2(CO)_3$ Structures

	3S-1 (C_2)		**3S-2** (C_1)		**3T-1** (C_1)		**3T-2** (C_1)	
	B3LYP	BP86	B3LYP	BP86	B3LYP	BP86	B3LYP	BP86
Fe_1-B_1	2.323	2.305	2.326	2.329	2.328	2.333	2.374	2.289
Fe_2-B_2	2.323	2.305	2.335	2.338	2.390	2.346	2.374	2.284
Fe_1-Fe_2	2.177	2.177	2.286	2.213	2.416	2.325	2.462	2.444
$-E$	3306.87873	3307.35339	3306.87454	3307.33271	3306.89009	3307.32423	3306.88823	3307.32331
ΔE	0.0	0.0	2.6	12.9	−7.1	18.2	−6.0	18.9
Nimg	none	none	none	none	none	none	none	none
$\langle S^2 \rangle$					2.58	2.07	2.62	2.08

Table 4. Total Energies (E in a.u.), Relative Energies (ΔE in kcal/mol), Fe−Fe and Fe−B Distances (in Å), Numbers of Imaginary Vibrational Frequencies (Nimg), and Spin Contaminations $\langle S^2 \rangle$ for the Eight $(C_4H_4BCH_3)_2Fe_2(CO)_2$ Structures

	2T-1 (C_2)		**2T-2** (C_1)		**2T-3** (C_{2h})		**2T-4** (C_1)	
	B3LYP	BP86	B3LYP	BP86	B3LYP	BP86	B3LYP	BP86
Fe_1-B_1	2.351	2.330	2.322	2.252	2.353	2.333	2.286	2.285
Fe_2-B_2	2.351	2.330	2.291	2.241	2.353	2.333	2.348	2.263
Fe_1-Fe_2	2.227	2.204	2.302	2.252	2.240	2.234	2.594	2.515
$-E$	3193.49251	3193.92757	3193.49376	3193.92444	3193.49209	3193.92408	3193.47962	3193.89698
ΔE	0.0	0.0	−0.8	2.0	0.3	2.2	8.1	19.2
Nimg	none	none	none	none	2(46i,24i)	1(69i)	none	none
$\langle S^2 \rangle$	2.51	2.09	2.70	2.07	2.50	2.09	2.72	2.08
	2S-1 (C_1)		**2S-2** (C_1)		**2S-3** (C_1)		**2S-4** (C_1)	
	B3LYP	BP86	B3LYP	BP86	B3LYP	BP86	B3LYP	BP86
Fe_1-B_1	2.254	2.218	2.590	2.517	2.281	2.249	2.270	2.285
Fe_2-B_2	2.300	2.276	2.341	2.329	2.249	2.222	2.313	2.308
Fe_1-Fe_2	2.348	2.347	2.142	2.096	2.477	2.439	2.206	2.147
$-E$	3193.47630	3193.92086	3193.45869	3193.91383	3193.46103	3193.90053	3193.45871	3193.92053
ΔE	10.2	4.2	21.2	8.6	19.8	17.0	21.2	4.4
Nimg	none	none	none	none	none	none	none	none

atoms a 17-electron configuration, corresponding to a binuclear triplet.

The ν(CO) frequencies for the $(C_4H_4BCH_3)_2Fe_2(CO)_4$ structures are listed in Table S50 of the Supporting Information. The terminal ν(CO) frequencies fall in the range 1917 to 2006 cm^{-1}, while the bridging ν(CO) frequencies are significantly lower in the range of 1822 to 1880 cm^{-1}.

3.1.3. $(C_4H_4BCH_3)_2Fe_2(CO)_3$. Four structures (two singlets and two triplets) for $(C_4H_4BCH_3)_2Fe_2(CO)_3$ have been found, including one triply bridged structure $(C_4H_4BCH_3)_2Fe_2(\mu\text{-}CO)_3$, two doubly bridged structures $(C_4H_4BCH_3)_2Fe_2(CO)(\mu\text{-}CO)_2$, and one singly bridged structure $(C_4H_4BCH_3)_2Fe_2(CO)_2(\mu\text{-}CO)$ (Figure 6 and Table 3). The B3LYP method predicts **3T-1** to be the global minimum (7.1 kcal/mol lower than **3S-1**) while the BP86 method predicts **3S-1** with C_2 symmetry to be the global minimum (18.2 kcal/mol lower than **3T-1**). Again this is an indication of the tendency for the B3LYP method to prefer triplet structures relative to the BP86 method.[52]

The $(C_4H_4BCH_3)_2Fe_2(CO)_3$ structure **3S-1** is a triply bridged structure (Figure 6 and Table 3). The Fe≡Fe distance in **3S-1** is 2.177 Å, consistent with the formal triple bond required to give both iron atoms the favored 18-electron configuration. The $(C_4H_4BCH_3)_2Fe_2(CO)_3$ structures **3S-2** and **3T-1** are doubly bridged structures. Structure **3S-2** lies energetically above **3S-1** by 2.6 kcal/mol (B3LYP) or 12.9 kcal/mol (BP86). In **3S-2** the Fe≡Fe distance is 2.286 Å (B3LYP) or 2.213 Å (BP86) consistent with the formal triple bond required to give both iron atoms the favored 18-electron configuration. The longer Fe≡Fe triple bond in **3S-2** relative to **3S-1** relates to the presence of three bridging CO groups in **3S-1** but only two bridging CO groups in **3S-2**.

The $(C_4H_4BCH_3)_2Fe_2(CO)_3$ structure **3T-1** lies below **3S-1** by −7.1 kcal/mol (B3LYP) or above **3S-1** by 18.2 kcal/mol (BP86) (Figure 6 and Table 3). In **3T-1**, the Fe═Fe distance is 2.416 Å (B3LYP) or 2.325 Å (BP86), which is significantly longer than that of **3S-2**. This suggests the Fe═Fe double bond required to give both iron atoms the 17-electorn configurations for a binuclear triplet.

The $(C_4H_4BCH_3)_2Fe_2(CO)_3$ structure **3T-2** is a singly bridged structure, lying below **3S-1** by 6.0 kcal/mol (B3LYP) or above **3S-1** by 18.9 kcal/mol (BP86) (Figure 6 and Table 3). The Fe═Fe distance in **3T-2** is 2.462 Å (B3LYP) or 2.444 Å (BP86), which is very similar to that in **3T-1**. This is consistent with the formal double bond needed to give both iron atoms the favored 17-electron configuration for a binuclear triplet.

The ν(CO) frequencies for the $(C_4H_4BCH_3)_2Fe_2(CO)_3$ structures are listed in Table S51 of the Supporting Information. The ν(CO) frequencies of the terminal CO groups fall in the range 1965 to 2005 cm^{-1}, while those for the bridging CO groups are appreciably lower in the range 1839 to 1902 cm^{-1}.

3.1.4. $(C_4H_4BCH_3)_2Fe_2(CO)_2$. The potential energy surface of $(C_4H_4BCH_3)_2Fe_2(CO)_2$ is significantly more complicated that those of the carbonyl richer derivatives $(C_4H_4BCH_3)_2Fe_2(CO)_n$ (n = 5, 4, 3), since a total of 8 different structures (Figure 7 and Table 4) are found within an energy range of ∼22 kcal/mol. All of these structures are genuine minima, except **2T-3**, which has two small imaginary vibrational frequencies at 46i and 24i cm^{-1}

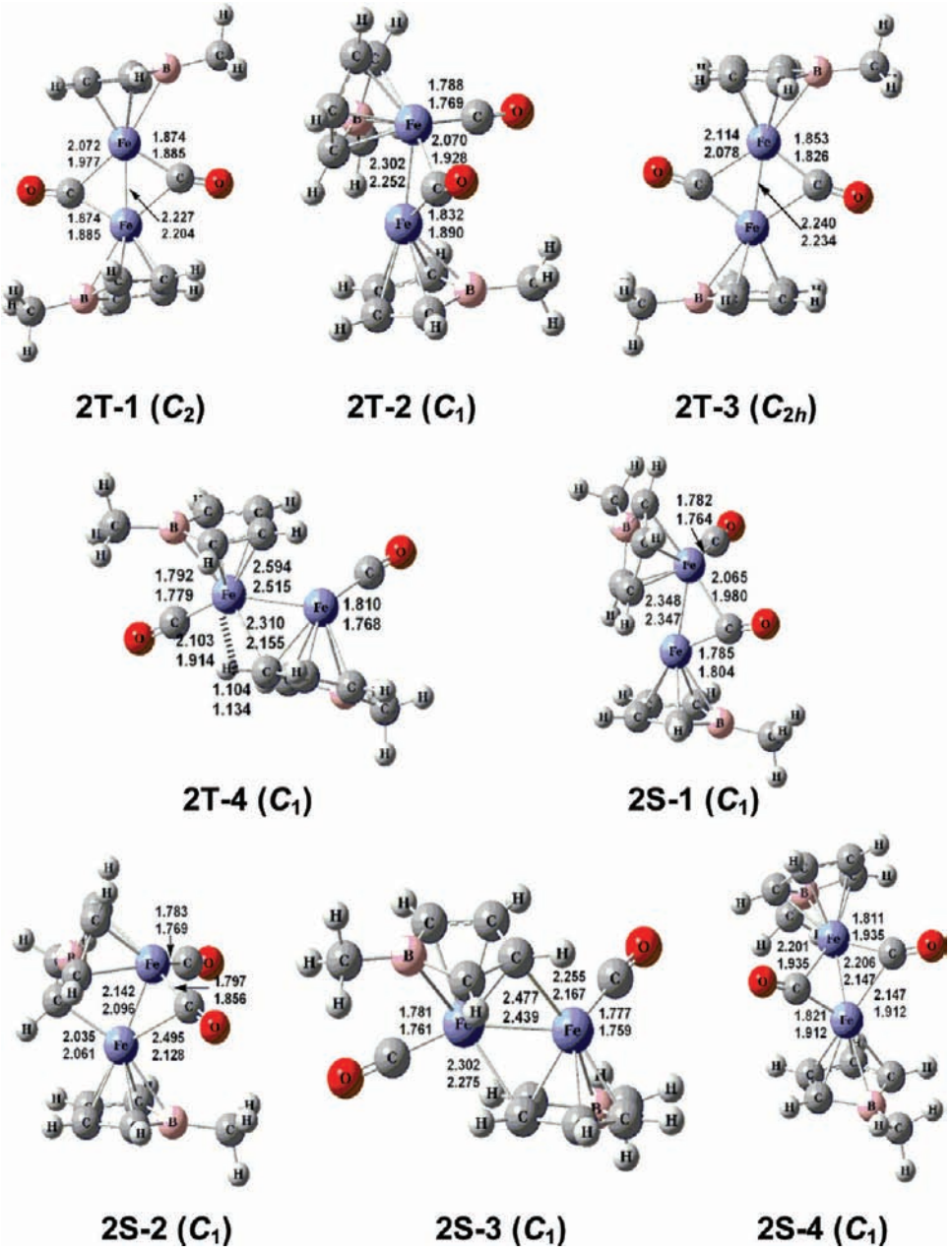

Figure 7. Optimized geometries for the eight $(C_4H_4BCH_3)_2Fe_2(CO)_2$ structures.

(B3LYP) or $69i\,cm^{-1}$ (BP86). Following the normal mode corresponding to the imaginary vibrational frequency of **2T-3** leads to **2T-1.**

The triplet $(C_4H_4BCH_3)_2Fe_2(CO)_2$ structures **2T-1** and **2T-2** are essentially energetically degenerate (Figure 7 and Table 4). Thus the B3LYP method predicts **2T-2** to be the global minimum (0.8 kcal/mol lower than **2T-1**), whereas the BP86 method predicts **2T-1** to be the global minimum (2.0 kcal/mol lower than **2T-2**). Structure **2T-3** is also close in energy to **2T-1** and **2T-2**, lying only 0.3 kcal/mol (B3LYP) or 2.2 kcal/mol (BP86) above **2T-1**. Structures **2T-1** (C_2) and **2T-3** (C_{2h}) are doubly bridged structures whereas structure **2T-2** is a singly bridged structure. The Fe≡Fe distances in the range 2.22 to 2.31 Å for the three structures **2T-1**, **2T-2**, and **2T-3** all suggest formal triple bonds thereby giving the iron atoms the 17-electron configurations for binuclear triplets.

Table 5. Bond Distances (in Å) and ν(CH) Frequencies by the BP86 Method for the **2T-4** (C_1) Structure

2T-4(C_1)	Fe−H	C−H	ν(CH), cm^{-1}
B3LYP	2.103	1.104	
BP86	1.914	1.134	2729

The singly bridged singlet $(C_4H_4BCH_3)_2Fe_2(CO)_2$ structures **2S-1** and **2S-2** lie 10.2 and 21.2 kcal/mol (B3LYP) or 4.2 and 8.6 kcal/mol (BP86), respectively, above **2T-1**. The Fe═Fe distance of 2.348 Å (B3LYP) or 2.347 Å (BP86) in **2S-1** is consistent with an Fe═Fe double bond, thereby giving each metal atom a 16-electron configuration. However, the Fe−Fe distances in the singly bridged structure **2S-2** and the doubly bridged structure **2S-4** are appreciably shorter at 2.142 Å (B3LYP) or 2.096 Å (BP86) for **2S-2** and 2.206 Å (B3LYP) or 2.147 Å (BP86) for **2S-4**. These short Fe−Fe distances can correspond to the Fe−Fe quadruple

bonds in **2S-2** and **2S-4** to give each iron atom the favored 18-electron configuration in each structure.

The remaining two $(C_4H_4BCH_3)_2Fe_2(CO)_2$ structures are the triplet **2T-4** and singlet **2S-3**, lying at the highest energies of the eight structures by the BP86 method (Figure 7 and Table 4). The carbonyl groups in these structures are terminal carbonyl groups. In **2S-3** two carbon atoms in each borole ring bridge both iron atoms. The Fe=Fe distance in **2S-3** of 2.477 Å (B3LYP) or 2.439 Å (BP86) is in the approximate range for a double bond. In **2T-4**, a carbon atom of one borole ring bridges the two iron atoms. One of the borole hydrogens in **2T-4** is an agostic hydrogen atom[56] with an unusually short Fe−H distance of 2.103 Å (B3LYP) or 1.914 Å (BP86) and an unusually long C−H distance of 1.104 Å (B3LYP) or 1.134 Å (BP86), leading to an unusually low ν(CH) frequency of 2729 cm^{-1} (BP86, Figure 7 and Table 5). This agostic C−H bond donates its two electrons to the iron atom not pentahapto bonded to the same methylborole ring. In this way both iron atoms in **2T-4** acquire the 17-electron configuration for a binuclear triplet in a structure with a polarized Fe=Fe double bond.

The ν(CO) frequencies for the $(C_4H_4BCH_3)_2Fe_2(CO)_2$ structures are listed in Table S52 of the Supporting Information. The terminal ν(CO) frequencies fall in the range 1938 to 1967 cm^{-1}, whereas those for the bridging CO groups are significantly lower in the range 1836 to 1874 cm^{-1}.

3.1.5. $(C_4H_4BCH_3)_2Fe_2(CO)$. Four structures are found for $(C_4H_4BCH_3)_2Fe_2(CO)$ (Figure 8 and Table 6). All of them are genuine minima. The triplet structures **1T-1** and **1T-2** have lower energies than the singlet structures **1S-1** and **1S-2**. Structures **1T-1**, **1T-2**, and **1S-1** are perpendicular structures that are related to the perpendicular structures previously reported[57] for some dimetallocenes such as $(C_5H_5)_2Ni_2$.

The triplet $(C_4H_4BCH_3)_2Fe_2(CO)$ structure **1T-1** (C_1) is the global minimum (Figure 8 and Table 6). It has a bridging carbon atom from a η^5-C_4H_4B ring and a bridging boron atom from the other borole ring, so structure **1T-1** is a perpendicular structure,[57] similar to Cp_2Ni_2. Structure **1T-2** is also a perpendicular structure and lies 6.9 kcal/mol (B3LYP) or 14.8 kcal/mol (BP86) in energy above **1T-1**. The iron−iron distances in **1T-1** and **1T-2** are 2.477 Å and 2.478 Å (B3LYP) or 2.416 Å and 2.337 Å (BP86), respectively, indicating that they are polarized Fe=Fe double bonds in accord thereby giving each iron a 17-electron configuration for a binuclear triplet.

The similar singlet perpendicular $(C_4H_4BCH_3)_2Fe_2(CO)$ structure **1S-1** with a terminal rather than bridging CO group, lies 21.4 kcal/mol (B3LYP) or 14.7 kcal/mol (BP86) above **1T-1** (Figure 8 and Table 6). The iron−iron distance in **1S-1** is 2.580 Å (B3LYP) or 2.492 Å (BP86). The singly bridged $(C_4H_4BCH_3)_2Fe_2(CO)$ structure **1S-2** lies 32.5 kcal/mol (B3LYP) or 22.3 kcal/mol (BP86) above **1T-1**. The Fe−Fe distance of 2.339 Å in **1S-2** (B3LYP) or 2.321 Å (BP86) is significantly shorter than that in **1S-1**.

Some short Fe−H distances and long C−H distances are found in all four $(C_4H_4BCH_3)_2Fe_2(CO)$ structures indicating the presence of agostic hydrogen atoms[56] (Figure 8 and Table 7). Accordingly, at least one unusually low ν(CH) vibrational frequency is predicted for each structure.

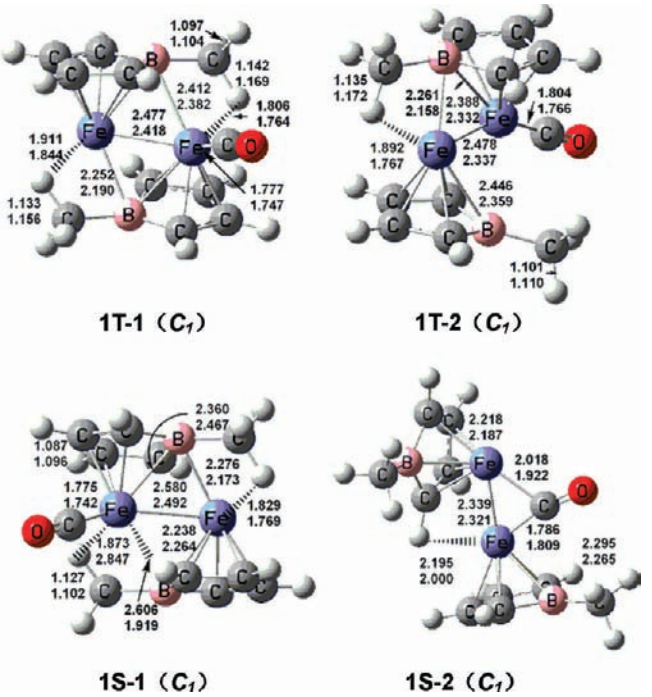

Figure 8. Optimized geometries for the four $(C_4H_4BCH_3)_2Fe_2(CO)$ structures.

Structure **1S-1** has two long C−H bonds. The B3LYP method predicts these long C−H bonds to be in the methyl group. However, the BP86 method predicts one long C−H bond in the methyl group and the other in a borole ring C−H bond.

3.2. Thermochemistry. Table 8 lists the dissociation energies of the following single carbonyl dissociation processes based on the global minimum structures:

$$(C_4H_4BCH_3)_2Fe_2(CO)_n \rightarrow (C_4H_4BCH_3)_2Fe_2(CO)_{n-1} + CO$$

In determining these dissociation energies, the fragments were allowed to relax.

The predicted dissociation energy for losing one CO group from $(C_4H_4BCH_3)_2Fe_2(CO)_5$ to give $(C_4H_4BCH_3)_2Fe_2(CO)_4$ is substantial, namely, 40.4 kcal/mol (B3LYP) or 46.2 kcal/mol (BP86). The energy for further dissociation of a CO group from $(C_4H_4BCH_3)_2Fe_2(CO)_4$ to give $(C_4H_4BCH_3)_2Fe_2(CO)_3$ is almost the same, namely, 45.1 kcal/mol (B3LYP) or 53.3 kcal/mol (BP86). However, the dissociation from $(C_4H_4BCH_3)_2Fe_2(CO)_3$ to $(C_4H_4BCH_3)_2Fe_2(CO)_2$ requires only 26.0 kcal/mol (B3LYP) or 16.3 kcal/mol (BP86). The CO dissociation energy from $(C_4H_4BCH_3)_2Fe_2(CO)_2$ to give $(C_4H_4BCH_3)_2Fe_2(CO)$ is 40.4 kcal/mol (B3LYP) or 38.5 kcal/mol (BP86). These carbonyl dissociation energies are in the typical range for metal carbonyl derivatives. Thus the experimental bond dissociation energies (BDEs) for $Ni(CO)_4$, $Fe(CO)_5$, and $Cr(CO)_6$ are 27 kcal/mol, 41 kcal/mol, and 37 kcal/mol, respectively.[58]

Table 9 lists the energies for the following disproportionation reactions:

$$2(C_4H_4BCH_3)_2Fe_2(CO)_n \rightarrow (C_4H_4BCH_3)_2Fe_2(CO)_{n+1} + (C_4H_4BCH_3)_2Fe_2(CO)_{n-1}$$

(56) Brookhart, M.; Green, M. L. H. *J. Organomet. Chem.* **1983**, *250*, 395.
(57) Xie, Y.; Schaefer, H. F.; King, R. B. *J. Am. Chem. Soc.* **2005**, *127*, 2818.
(58) Sunderlin, L. S.; Wang, D.; Squires, R. R. *J. Am. Chem. Soc.* **1993**, *115*, 12060.

Table 6. Total Energies (E in a.u.), Relative Energies (ΔE in kcal/mol), Fe−Fe and Fe−B Distances (in Å), Numbers of Imaginary Vibrational Frequencies (Nimg), Spin Expectation Values $\langle S^2 \rangle$, ν(CO) Vibrational Frequencies (in cm^{-1}), and Corresponding Infrared Intensities (km/mol, in Parentheses) for the $(C_4H_4BCH_3)_2Fe_2(CO)$ Structures

	1T-1 (C_1)		**1T-2** (C_1)		**1S-1** (C_1)		**1S-2** (C_1)	
	B3LYP	BP86	B3LYP	BP86	B3LYP	BP86	B3LYP	BP86
Fe_1-B_1	2.339	2.260	2.388	2.332	2.360	2.407	2.218	2.187
Fe_2-B_2	2.291	2.189	2.446	2.359	2.238	2.264	2.295	2.265
Fe_1-Fe_2	2.477	2.416	2.478	2.337	2.580	2.492	2.339	2.321
$-E$	3080.12035	3080.53706	3080.10935	3080.51350	3080.08630	3080.51357	3080.06855	3080.50160
ΔE	0.0	0.0	6.9	14.8	21.4	14.7	32.5	22.3
Nimg	none	none	none	none	none	none	none	none
$\langle S^2 \rangle$	2.32	2.13	3.07	2.10	0.00	0.00	0.00	0.00
ν(CO)		1933(902)		1931(1016)		1929(1062)		**1776(521)**

Table 7. Bond Distances (in Å) and ν(CH) Frequencies (in cm^{-1}) by the BP86 Method for the $(C_4H_4BCH_3)_2Fe_2(CO)$ Structures

	1T-1 (C_1)		**1T-2** (C_1)		**1S-1** (C_1)		**1S-2** (C_1)	
	B3LYP	BP86	B3LYP	BP86	B3LYP	BP86	B3LYP	BP86
Fe−H	1.806	1.767	1.892	1.767	1.829, 1.873	1.769, 1.919	2.195	2.000
C−H	1.142	1.172	1.135	1.172	1.127, 1.137	1.138, 1.171	1.098	1.122
ν(CH)		2331		2331		2334, 2687		2859

Table 8. Dissociation Energies (kcal/mol) of $(C_4H_4BCH_3)_2Fe_2(CO)_n$.for the Successive Removal of a Carbonyl Group

	B3LYP	BP86
$(C_4H_4BCH_3)_2Fe_2(CO)_5 \rightarrow (C_4H_4BCH_3)_2Fe_2(CO)_4 + CO$	40.4	46.2
$(C_4H_4BCH_3)_2Fe_2(CO)_4 \rightarrow (C_4H_4BCH_3)_2Fe_2(CO)_3 + CO$	45.1	53.3
$(C_4H_4BCH_3)_2Fe_2(CO)_3 \rightarrow (C_4H_4BCH_3)_2Fe_2(CO)_2 + CO$	26.0	16.3
$(C_4H_4BCH_3)_2Fe_2(CO)_2 \rightarrow (C_4H_4BCH_3)_2Fe_2(CO) + CO$	40.4	38.5

Table 9. Energies (kcal/mol) for the Disproportionation Reactions $2(C_4H_4BCH_3)_2Fe_2(CO)_n \rightarrow (C_4H_4BCH_3)_2Fe_2(CO)_{n+1} + (C_4H_4BCH_3)_2Fe_2(CO)_{n-1}$

	B3LYP	BP86
$2(C_4H_4BCH_3)_2Fe_2(CO)_4 \rightarrow (C_4H_4BCH_3)_2Fe_2(CO)_5 + (C_4H_4BCH_3)_2Fe_2(CO)_3$	−4.6	−7.1
$2(C_4H_4BCH_3)_2Fe_2(CO)_3 \rightarrow (C_4H_4BCH_3)_2Fe_2(CO)_4 + (C_4H_4BCH_3)_2Fe_2(CO)_2$	19.1	37.0
$2(C_4H_4BCH_3)_2Fe_2(CO)_3 \rightarrow (C_4H_4BCH_3)_2Fe_2(CO)_5 + (C_4H_4BCH_3)_2Fe_2(CO)$	19.2	44.8
$2(C_4H_4BCH_3)_2Fe_2(CO)_2 \rightarrow (C_4H_4BCH_3)_2Fe_2(CO)_3 + (C_4H_4BCH_3)_2Fe_2CO$	−14.4	−22.1

The energies of the reactants and products are all those of the global minima, which are different for the B3LYP and BP86 functionals. The tricarbonyl $(C_4H_4BCH_3)_2Fe_2(CO)_3$ is seen to be thermodynamically viable with respect to disproportionation into $(C_4H_4BCH_3)_2Fe_2(CO)_5$ + $(C_4H_4BCH_3)_2Fe_2(CO)$ or $(C_4H_4BCH_3)_2Fe_2(CO)_4$ + $(C_4H_4BCH_3)_2Fe_2(CO)_2$ (Table 9). However, the tetracarbonyl $(C_4H_4BCH_3)_2Fe_2(CO)_4$ and particularly the dicarbonyl $(C_4H_4BCH_3)_2Fe_2(CO)_2$ are seen to be unstable with respect to analogous disproportionation reactions.

4. Discussion

The methylborole ligands in all of the $(C_4H_4BCH_3)_2Fe_2(CO)_n$ (n = 5, 4, 3) structures are all pentahapto coordinated with both Fe−B and Fe−C interactions of the iron centers to the methylborole ligands. The Fe−B bonding distances in these structures typically fall in the range 2.3 to 2.4 Å. Thus, the boron atom in the methylborole ligand is an active participant in the ligand−metal bonding.

The lowest energy $(C_4H_4BCH_3)_2Fe_2(CO)_5$ structures are the singly bridged structures **5S-1** and **5S-2** with trans and cis orientations of the methylborole ligands, respectively (Figure 4). A singly bridged structure was previously predicted[59] to be the lowest energy structure for the cyclobutadieneiron complex $(C_4H_4)_2Fe_2(CO)_5$. However, the predicted Fe−Fe single bond distances of ~2.85 Å in the singly bridged $(C_4H_4BCH_3)_2Fe_2(CO)_4(\mu\text{-CO})$ structures are significantly longer than the ~2.76 Å Fe−Fe single bond distance in the singly bridged cyclobutadieneiron complex. The lowest energy predicted structure[60] of the isoelectronic $(C_5H_5)_2Mn_2(CO)_5$ is also a singly bridged structure with a Mn−Mn single bond distance of ~2.83 Å very similar to that in the $(C_4H_4BCH_3)_2Fe_2(CO)_4(\mu\text{-CO})$ structures **5S-1** and **5S-2**. The lowest lying triplet $(C_4H_4BCH_3)_2Fe_2(CO)_5$ structure lies > 35 kcal/mol above the lowest lying singlet $C_4H_4BCH_3)_2Fe_2(CO)_5$ structure. Thus, triplet $(C_4H_4BCH_3)_2Fe_2(CO)_5$ structures are not likely to be chemically significant.

The lowest lying $(C_4H_4BCH_3)_2Fe_2(CO)_4$ structures are doubly bridged structures. The Fe═Fe distances in the range 2.43 to 2.64 Å in the singlet $(C_4H_4BCH_3)_2Fe_2(CO)_2(\mu\text{-CO})_2$ structures are significantly shorter than the Fe−Fe distances of ~2.85 Å in the singlet $(C_4H_4BCH_3)_2Fe_2(CO)_4(\mu\text{-CO})$ structures discussed above. This is consistent with the formal Fe═Fe double bond in the singlet $(C_4H_4BCH_3)_2Fe_2(CO)_2(\mu\text{-CO})_2$ structures required to give the iron atoms the favored 18-electron configuration. A similar collection of doubly bridged structures is found for the analogous cyclobutadiene iron carbonyl[59] and cyclopentadienylmanganese carbonyl[60]

(59) Wang, H.; Xie, Y.; King, R. B.; Schaefer, H. F. *Organometallics* **2008**, *27*, 3113.

(60) Zhang, X.; Li, Q.-S.; Xie, Y.; King, R. B.; Schaefer, H. F. *Organometallics* **2008**, *27*, 61.

systems. The tetracarbonyl $(C_4H_4BCH_3)_2Fe_2(CO)_4$ is predicted to be thermodynamically unstable with respect to disproportionation into $(C_4H_4BCH_3)_2Fe_2(CO)_5 + (C_4H_4BCH_3)_2Fe_2(CO)_3$ and thus does not appear to be a viable synthetic objective.

The tricarbonyls are of particular interest since both of the permethylated derivatives $[\eta^4\text{-}(CH_3)_4C_4]_2Fe_2(\mu\text{-}CO)_3$ and $[\eta^5\text{-}(CH_3)_5C_5]_2Mn_2(\mu\text{-}CO)_3$ have been synthesized.[17−20] Infrared spectroscopy and X-ray crystallography indicate structures with three bridging carbonyl groups and short M≡M distances similar to the lowest energy structures predicted in the theoretical studies. The short M≡M distances suggest the formal triple bonds required to give the central metal atoms the favored 18-electron configurations. The lowest energy $(C_4H_4BCH_3)_2Fe_2(CO)_3$ structure **3S-1** (Figure 6) is predicted to be a completely analogous triply bridged structure. The predicted Fe≡Fe triple bond distance of 2.17 Å in $(\eta^5\text{-}C_4H_4BCH_3)_2Fe_2(\mu\text{-}CO)_3$ (**3S-1**) is very similar to the 2.15 Å Fe≡Fe distance predicted[59] for $(\eta^4\text{-}C_4H_4)_2Fe_2(\mu\text{-}CO)_3$ and the 2.17 Å Mn≡Mn distance found by X-ray crystallography[21] in $[\eta^5\text{-}(CH_3)_5C_5]_2Mn_2(\mu\text{-}CO)_3$. The $(C_4H_4BCH_3)_2Fe_2(CO)_3$ structure **3S-1** is predicted to be thermodynamically viable with respect to disproportionation into $(C_4H_4BCH_3)_2Fe_2(CO)_4 + (C_4H_4BCH_3)_2Fe_2(CO)_2$ and thus appears to be a viable synthetic objective.

A singlet $(\eta^5\text{-}C_4H_4BCH_3)_2Fe_2(CO)_2$ structure requires a formal Fe−Fe quadruple bond to give each iron atom the favored 18-electron configuration. Instead, the two lowest energy $(\eta^5\text{-}C_4H_4BCH_3)_2Fe_2(CO)_2$ structures **2T-1** and **2T-2** (Figure 7) are doubly bridged triplets with predicted Fe≡Fe triple bond distances in the range 2.2 to 2.3 Å. The longer Fe≡Fe triple bond distances in $(\eta^5\text{-}C_4H_4BCH_3)_2Fe_2(\mu\text{-}CO)_2$ relative to $(\eta^5\text{-}C_4H_4BCH_3)_2Fe_2(\mu\text{-}CO)_3$ can be related to the presence of two carbonyl bridges in the former but three carbonyl bridges in the latter. Similar doubly bridged triplet structures[59,60] are predicted for $(C_4H_4)_2Fe_2(\mu\text{-}CO)_2$ and $(C_5H_5)_2Mn_2(\mu\text{-}CO)_2$.

Structures with bridging methylborole ligands and agostic hydrogen atoms[56] are also found for $(C_4H_4BCH_3)_2Fe_2(\mu\text{-}CO)_2$. Thus, in **2T-4** (Figure 7) one of the borole ligands bridges the two iron atoms by functioning as a pentahapto ligand to one iron atom and forming an agostic C−H→Fe bond to the other iron atom. The resulting Fe−H interaction is characterized by a short Fe−H distance of 2.103 Å (B3LYP) or 1.914 Å (BP86) and an unusually low ν(CH) frequency of 2729 cm^{-1} (Table 5). Bridging methylborole ligands are also found in the singlet $(C_4H_4BCH_3)_2Fe_2(\mu\text{-}CO)_2$ structures **2S-2** and **2S-3**. In fact structure **2S-3** may be considered as a "slipped perpendicular" structure with two bridging methylborole ligands.

Blind application of the 18-electron rule suggests that a singlet monocarbonyl $(C_4H_4BCH_3)_2Fe_2(CO)$ might have a very short Fe−Fe quintuple bond. Instead the lowest energy structures are perpendicular structures with a terminal carbonyl ligand, bridging borole ligands, and at least one agostic hydrogen atom[56] from the methyl group of the methylborole ligand to an iron atom (Figure 8). Thus, the methyl substituent in the methylborole ligand is not an innocent bystander but instead participates in the metal−ligand bonding in these highly unsaturated systems. These agostic hydrogen atoms provide a mechanism for the highly unsaturated iron atoms to receive two electrons from one of the borole C−H bonds.

5. Summary

The lowest energy structures of the binuclear methylborole iron carbonyls $(C_4H_4BCH_3)_2Fe_2(CO)_n$ (n = 5, 4, 3) resemble those of the related $(C_5H_5)_2Mn_2(CO)_n$ and $(C_4H_4)_2Fe_2(CO)_n$ derivatives. The short Fe−B distances in all of these structures indicate that the methylborole ligand is a pentahapto ligand involving the boron atom, as well as the two C=C double bonds. The lowest energy $(C_4H_4BCH_3)_2Fe_2(CO)_5$ structures have a single bridging carbonyl group and an Fe−Fe distance consistent with a formal single bond. The lowest energy $(C_4H_4BCH_3)_2Fe_2(CO)_4$ structures have two bridging carbonyl groups and an Fe=Fe distance suggesting a formal double bond. Analogously the lowest energy $(C_4H_4BCH_3)_2Fe_2(CO)_3$ have three bridging carbonyl groups and a very short Fe≡Fe distance suggesting a formal triple bond. The tetracarbonyl $(C_4H_4BCH_3)_2Fe_2(CO)_4$ is predicted to be thermodynamically unstable toward disproportionation into $(C_4H_4BCH_3)_2Fe_2(CO)_5 + (C_4H_4BCH_3)_2Fe_2(CO)_3$ whereas the tricarbonyl is thermodynamically viable toward analogous disproportionation.

The structures of the more highly unsaturated methylborole iron carbonyls $(C_4H_4BCH_3)_2Fe_2(CO)_n$ (n = 2, 1) exhibit some new features not found in their $(C_5H_5)_2Mn_2(CO)_n$ and $(C_4H_4)_2Fe_2(CO)_n$ analogues. The hydrogen atoms in the methylborole ligand can interact directly with the highly unsaturated iron atoms as agostic hydrogen atoms. In addition, the lowest energy $(C_4H_4BCH_3)_2Fe_2(CO)$ structures are "slipped perpendicular" structures with bridging methyl borole ligands, a terminal carbonyl group, and agostic CH_3→Fe interactions involving the methyl hydrogens. Thus, in these systems the methyl substituent in the methylborole ligand chosen in this work is not an "innocent bystander" but instead participates in the metal−ligand bonding.

Acknowledgment. We are indebted to the Science and Technology Support Program Project of Sichuan Province (2009JY0140), the Research Fund of Key Disciplines of Atomic and Molecular Physics, Xihua University, China, and the U.S. National Science Foundation (Grant CHE-0716718) for the support of this research. We also thank Professor Hongyan Wang for her help and discussions.

Supporting Information Available: Tables S1 to S24: Atomic coordinates of the optimized structures for the $(C_4H_4BCH_3)_2Fe_2(CO)_n$ (n = 5, 4, 3, 2, 1) complexes; Tables S25 to S48: Harmonic vibrational frequencies (in cm^{-1}) and infrared intensities (in parentheses in km/mol) for the $(C_4H_4BCH_3)_2Fe_2(CO)_n$ (n = 5, 4, 3, 2, 1) complexes; Table S49 to S52: The ν(CO) vibrational frequencies and corresponding infrared intensities predicted for the $(C_4H_4BCH_3)_2Fe_2(CO)_n$ (n = 5, 4, 3, 2) structures using the BP86 method; complete Gaussian reference (reference 50). This material is available free of charge via the Internet at http://pubs.acs.org.